Dual-capillary dilatometer for density measurements of supercooled water

Aleš Blahut[1*], *Jiří* Hykl[1], *Pavel* Peukert[1], and *Jan* Hrubý[1]

[1]Institute of Thermomechanics of the Czech Academy of Sciences, Dolejškova 1402, 182 00 Prague 8, Czech Republic

Abstract. An apparatus tailored to accurate density measurements of supercooled water, i.e. liquid water in a metastable state below the freezing point temperature, was recently developed at the Institute of Thermomechanics of the Czech Academy of Sciences. The apparatus, dual-capillary dilatometer, is described, together with the measurement procedure and the evaluation methodology. The primary result of the dual-capillary method are relative densities with respect to the density at a reference temperature and given pressure. In order to calculate absolute densities, densities at the reference temperature as a function of pressure are needed. For calculation of such pressure dependence of density, so called thermodynamic integration involving literature thermodynamic data and our experimental results is used. The dual-capillary dilatometer was successfully employed in density measurements of ordinary water, heavy water and seawater. The data in the temperature range from 238.15 to 303.15 K at pressures from atmospheric up to 200 MPa are presented and compared with respective IAPWS formulations of thermodynamic properties. The data for ordinary water are also compared with an accurate equation of state for supercooled water of Holten et al. (2014) revealing good mutual agreement. The expanded uncertainty of relative densities acquired by means of the dual-capillary method is estimated to be lower than 50 ppm.

1 Introduction

Recently, an apparatus for accurate density measurements of supercooled water, i.e. liquid water in a metastable state below the freezing point temperature, was developed at the Institute of Thermomechanics of the Czech Academy of Sciences [1, 2]. The primary aim of the apparatus was to provide reliable density data with low uncertainty for supercooled water not only at atmospheric pressure but also at high pressures and contribute thus to the ongoing research of metastable water.

Usually, the measurement of thermophysical properties of water in the supercooled state is a compromise between accuracy and a level of supercooling. The persistence of liquid state below the freezing point temperature has a probabilistic character. In order to trigger freezing, formation of a nucleation center is needed. The purer is a liquid, the lower is its volume, and the smaller is the departure from the freezing point temperature, the creation of such nucleation center is less probable. In other words, more time is available for measurement before the liquid freezes.

The small volume of liquid for various measurement techniques is usually achieved in capillaries with small inner diameter [3, 4] or in emulsions, e.g., where water is dispersed in the form of small droplets in a hydrophobic solvent [5, 6]. However, decreasing the volume pronounces surface effects which distort the recognition of bulk properties. Some studies were discussing a possible influence of capillary inner diameter on results of density measurements with supercooled water [3, 7]. It seems that water enclosed in a capillary with diameter of around 300 μm represents well bulk water, while keeping considerable supercooling capabilities at the same time [3]. Measurements carried out in emulsions approach the homogeneous nucleation limit but they are less accurate than measurements in capillaries because of uncertainty connected with subtracting emulsion matrix properties.

Highlights of the developed apparatus, dual-capillary dilatometer, are the high accuracy exceeding previous measurements in supercooled region and the possibility of measurements at high pressures. The estimated relative expanded uncertainty of measurements is lower than $5 \cdot 10^{-5}$. On the other hand, compared to literature data, e.g. [3, 5], only moderate level of superccoling was achieved (approximately 20 K below freezing point temperature).

Even though the dual-capillary dilatometer was specifically designed for ordinary water, it can be used for wider variety of substances. Straightforward is the application for water isotopologues or aqueous solutions. Up to this date the apparatus was successfully employed within three measurement campaigns including ordinary water (H_2O), heavy water (D_2O) [8] and a sample of IAPSO seawater standard. The results for D_2O together with preliminary results for H_2O and seawater standard are presented in this paper.

* Corresponding author: blahut@it.cas.cz

© The Authors, published by EDP Sciences. This is an open access article distributed under the terms of the Creative Commons Attribution License 4.0 (http://creativecommons.org/licenses/by/4.0/).

2 Measurement principle

Measurement method is based on measuring height changes of a liquid column situated inside a capillary. The change of the column height is induced by switching temperature of liquid from a reference temperature T_{ref} to a temperature of interest T. Due to practical reasons, the change of temperature is realized only for a part of the capillaries situated in a heat exchanger, as schematically depicted on the right hand side of Fig. 1. The left hand side of the figure illustrates a zone held at a constant reference temperature. In reality, the zone corresponds to an optical cell which enables observation of the column heights through high-pressure sapphire windows. In order to eliminate an effect of the transition zone between the optical cell and the heat exchanger, two capillaries are used: a long one (L) and a short one (S). Mercury is used in both capillaries as a movable plug separating the investigated liquid from a pressurizing gas. At the same time, mercury serves also as a contrast substance for better identification of the position of liquid menisci. Two measurement states with different menisci positions are distinguished in Fig. 1 by black and gray colors. Δa represents the length difference of two capillaries, Δz_S and Δz_L stand for menisci position differences in respective capillaries.

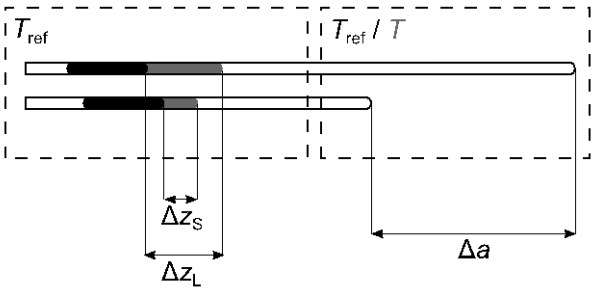

Fig. 1. Illustration of the dual-capillary method principle (rotated 90 ° counterclockwise compared to the position of capillaries in the apparatus).

The primary result of the measurement using dual-capillary method is the relative density η, i.e. the ratio of density at the temperature of interest T and density at the reference temperature T_{ref} at a given pressure p:

$$\eta(T, p) = \frac{\rho(T, p)}{\rho(T_{ref}, p)}. \quad (1)$$

Based on the measurement of menisci position differences, Δz_S, Δz_L, and fixed length difference of capillaries, Δa, the relative density can be calculated in first approximation with the idealized equation

$$\eta = 1 - \frac{\Delta z_L - \Delta z_S}{\Delta a}. \quad (2)$$

It should be noted that the differences Δz_S and Δz_L are negative in case of liquid contraction.

In order to improve accuracy of the measurement description, several correction factors are considered [8]. The corrective terms stand for dilation of capillary material (fused silica), dilation of a reference glass scale, variation of cross-section area of capillaries along their length [2], or hydrostatic pressure correction. Variation of temperature and pressure from nominal values is also considered.

3 Description of apparatus and measurement procedure

Since a design of apparatus was introduced in detail before [1, 8], here only a brief description is given.

Long and short capillaries are manufactured of fused silica, which offers a very low coefficient of thermal expansion, compared, e.g., to the borosilicate glass or stainless steel commonly used in experiments with supercooled water. Prior to the measurements both capillaries are sealed tightly at the one end and filled with liquid using a special device [1]. During the filling procedure a sample is degassed by controlled stepwise evacuation while being stirred with a magnetic bar. Consequently, the degassed sample is sucked into evacuated capillary. Finally, a small mercury column is introduced in the capillary from the open end in order to prevent contact of liquid with a pressurization gas during the measurement.

For the measurement, capillaries are fixed vertically inside a high-pressure containment which consists of thermostated high-pressure optical cell and two tube heat exchangers. The pressurization is carried out with a help of inert gas (nitrogen) whereas the capillaries are pressurized both from inner and outer side thanks to the movable mercury plug. The actual state of apparatus enables density measurements up to 200 MPa.

Locations of menisci in capillaries are observed through sapphire windows using high-resolution CCD camera (piA2400-12gm, Basler) equipped with telecentric lens (TECHSPEC®, Edmund Optics). The resolution of camera is calibrated by means of in-situ installed contact reticle (Edmund Optics) with declared line to line accuracy 2 μm. Acquired images are semi-automatically evaluated with an image processing code yielding positions of menisci in capillaries z_L and z_S.

The measurements are carried out at isobaric conditions. In order to obtain relative density for a certain temperature, two measurement states have to be realized. In reference state the entire vertical profile of capillaries is maintained at the reference temperature T_{ref}, while at measuring state only the bottom heat exchanger is switched to the temperature of interest T. The main reason of switching procedure is to avoid freezing when temperature of interest is within the supercooled region. After a certain time needed for stabilization, camera images are acquired and temperature switched quickly back to T_{ref}. Usually three images are taken per each measurement state.

Temperatures at different locations of apparatus are monitored with Pt100 sensors connected to thermometry bridge (CTR6500, ASL). Pressure is measured using accurate transducers Digiquiartz® 415K-101 or 430K-101 (Paroscientific, Inc.) depending on pressure range.

4 Thermodynamic integration

As mentioned before, the dual capillary dilatometer provides relative densities. In order to convert relative densities into absolute ones, density at the reference temperature as a function of temperature is needed. E.g., available reference equations of states can be used for this purpose. However, within our studies with water, heavy water and seawater, an alternate approach called thermodynamic integration was used. The approach benefits from availability of highly accurate sound speed data for selected liquids [9-12]. In this case the thermodynamic integration may yield more accurate densities at high pressures compared to contemporary reference equations of state.

For the determination of reference densities, the following pair of differential equations needs to be solved.

$$\left(\frac{\partial \rho}{\partial p}\right)_T = \frac{1}{w^2} + T\frac{\alpha_p^2}{c_p}, \tag{3}$$

$$\left(\frac{\partial c_p}{\partial p}\right)_T = -\frac{T}{\rho}\beta_p . \tag{4}$$

In these equations, w is speed of sound, c_p is specific isobaric heat capacity, α_p denotes isobaric expansivity, and β_p is the second order thermal expansion coefficient. In favorable cases, accurate values of w are available in the literature at the conditions of interest, i.e. at the reference temperature and simultaneously as a function of pressure. Heat capacity and density at the reference temperature and atmospheric pressure are needed as initial conditions for the integration. Concerning liquids involved in this work, respective reference equations recommended by IAPWS [13-15] can be sufficiently used for calculation of these single point data. Particular values of isobaric expansivity α_p or the second order thermal expansion coefficient β_p can be calculated from experimental relative densities as follows

$$\alpha_p = \frac{1}{v}\left(\frac{\partial v}{\partial T}\right)_p = -\frac{1}{\eta}\left(\frac{\partial \eta}{\partial T}\right)_p , \tag{5}$$

$$\beta_p = \frac{1}{v}\left(\frac{\partial^2 v}{\partial T^2}\right)_p = 2\alpha_p^2 - \frac{1}{\eta}\left(\frac{\partial^2 \eta}{\partial T^2}\right)_p . \tag{6}$$

There are many options how to solve the set of differential equations Eq. 3 and Eq. 4. In our studies numerical integration using fourth order Runge-Kutta method was applied.

5 Results and discussion

Dual capillary dilatometer was used for density measurements with ordinary water, heavy water and IAPSO standard seawater sample. Relative expanded uncertainties (k = 2) of primary experimental results, i.e. relative densities, are estimated to be lower than $5 \cdot 10^{-5}$.

5.1 Specification of liquid samples

Ordinary water was prepared using two step purification system consisting of reverse osmosis (Rowapur) and purification unit (Neptune Analytical). According to the unit specification, outlet water reaches resistivity 18.2 MΩ·cm, is free of particles larger than 0.2 μm and has an organic carbon content below $5 \cdot 10^{-9}$.

Heavy water (D_2O) sample was purchased from Sigma-Aldrich. According to the certificate of analysis provided by the supplier for particular batch, deuterium fraction among hydrogen isotopes was declared to be higher than 0.9999. Heavy water sample was used without any purification, except for degassing during the capillary filling procedure.

IAPSO Standard Seawater (OSIL, batch 161) with certified practical salinity 34.995 was used for density measurements. However, during the controlled degassing procedure the salinity gently increased due to evaporation of pure water. Based on a VLE calculation, the practical salinity of seawater involved in measurements was estimated to be 35.016 which corresponds to the absolute salinity 35.181 g kg^{-1} [16].

5.2 Absolute density results

Density results for all investigated liquids are shown in graphical form in figures Fig. 2 to Fig. 4. Resulting densities were obtained by combining experimental relative densities and reference density values from thermodynamic integration as follows

$$\rho(T, p) = \rho_{\mathrm{TD}}(p)\,\eta(T, p), \tag{7}$$

where ρ_{TD} denotes density values obtained by thermodynamic integration at a reference temperature T_{ref}. For ordinary water and seawater T_{ref} = 293.15 K, whereas heavy water experiments were carried out with different reference temperature 298.15 K.

In all these figures open circles mark nominal experimental temperatures and gray dashed lines represent melting curves of associated liquids.

As can be seen, the measurements carried out with water covers the broadest pressure range, from atmospheric pressure up to 200 MPa. Also for ordinary water most efforts were made to achieve the deepest supercooling possible. Because these efforts usually lead to destruction of laboriously prepared capillaries, decreasing the temperature to a limit was done only for several isobars. The deepest supercooling, 22 K below the freezing point, was achieved at 100 MPa. In case of usual measurements, the range of supercooling varied roughly between 10 and 15 K.

The general feature for water, heavy water and seawater is an existence of density maximum and the fact that this maximum vanishes with increasing pressure, particularly temperature of maximum density moves to lower temperatures as discussed in section 5.4.

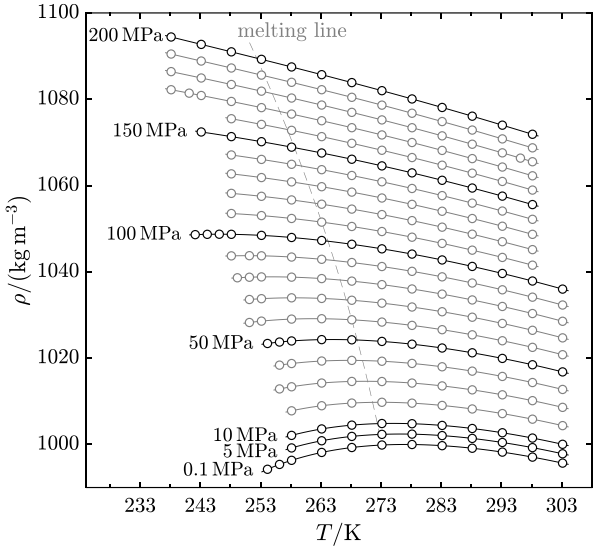

Fig. 2. Density isobars of ordinary water.

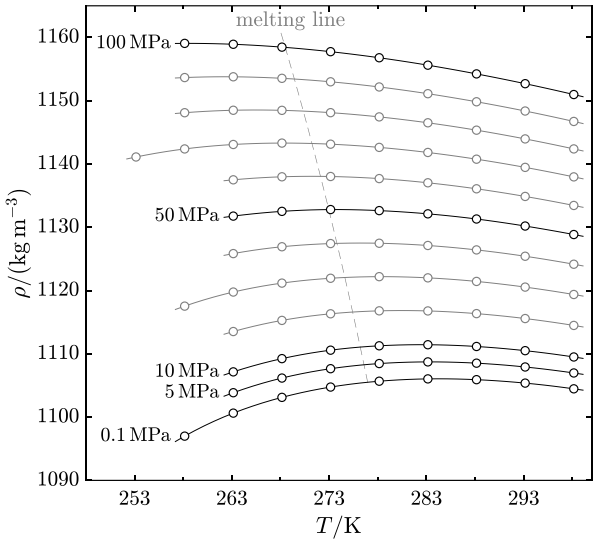

Fig. 3. Density isobars of heavy water.

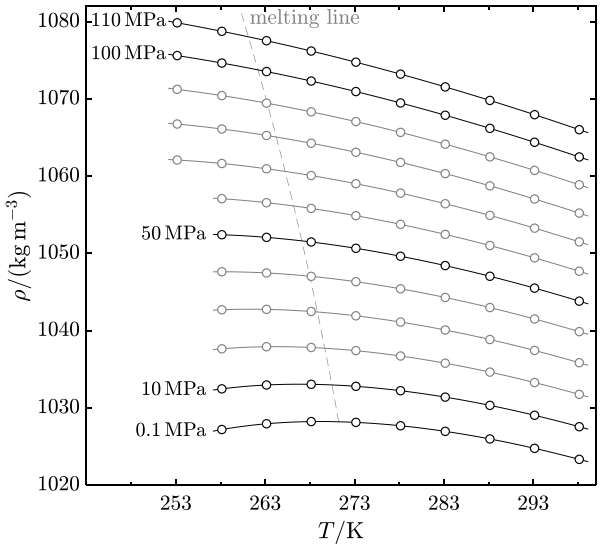

Fig. 4. Density isobars of standard seawater (absolute salinity 35.16504 g·kg^{-1}).

5.3 Comparison with reference equations of state

In this section the new experimental densities are compared with relevant reference equations of state (EoS). For pure water, results are compared with two equations, namely IAPWS-95 [13] and EoS of Holten et al. [17] from 2014, which is specifically designed to describe supercooled region. Results of heavy water are compared to recent EoS of Herrig et al. [14] and seawater densities are confronted with TEOS-10 equation [18], which is principally based on EoS developed by Feistel [15].

In Fig. 5 and Fig. 6 experimental densities are compared to IAPWS-95 formulation and Holten EoS, respectively. The agreement with Holten equation is very good, up to 120 MPa Holten equation even agrees with our densities within relative expanded uncertainty of our data (~5·10^{-5}). The mutual agreement with IAPWS-95 in supercooled region is somehow poorer, the deviations are more pronounced with increasing pressure.

What is not visible due to limited resolution is the fact, that Holten EoS also agree better than IAPWS-95 with our data at 273.15 K and above at high pressures. In particular, differences from Holten EoS for all experimental pressures are within ±20·10^{-6}, whereas in case of IAPWS-95 the differences range within ±60·10^{-6}.

It should be noted that at atmospheric pressure above melting point the Holten equation provides the same densities as IAPWS-95, but differences between these equations are increasing with pressure. At high pressures in the limited temperature range of our studies Holten equation may be considered more reliable than IAPWS-95, e.g., because more accurate speed of sound data was used within equation development and quality of speed of sound data influences the quality of density derivative with respect to pressure (as can be inferred from Eq. 3 in section 4).

The excellent agreement with Holten equation above melting point curve proves to certain extent reliability of our results.

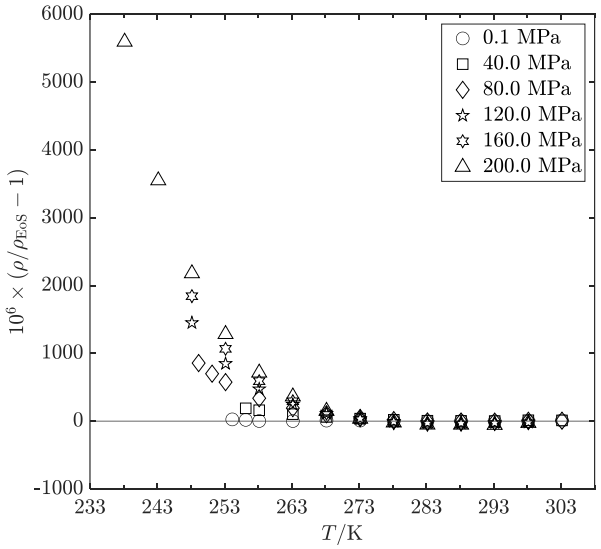

Fig. 5. Relative deviations of H_2O densities from this work from densities calculated with IAPWS-95 formulation [13].

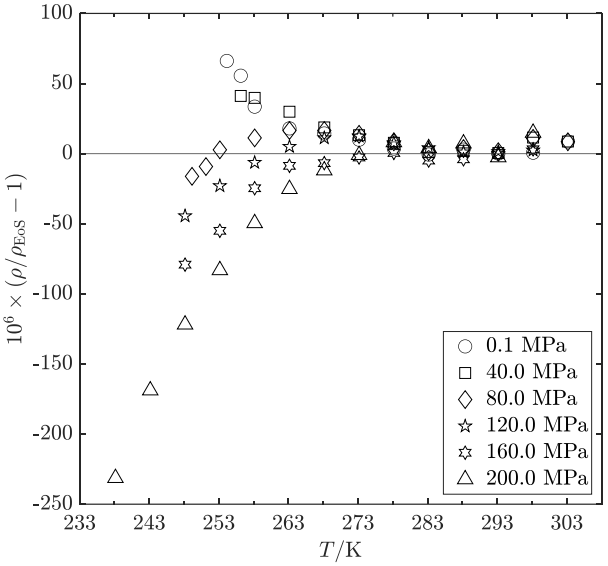

Fig. 6. Relative deviations of H_2O densities from this work from densities calculated wtih Holten EoS [17] for several isobars.

Recently developed equation for heavy water [14] agrees quite well with our data as can be seen in Fig. 7. However, it should be noted that our preliminary results were used for development of this equation. Comparing our density data with the equation in detail, there is an obvious difference in slope of density vs temperature from 273.15 K to 298.15 K. This deviation seems to be systematic for all experimental pressures. As discussed previously [8], the deviation is probably an artifact of the equation. The slope of density vs temperature of our data at the atmospheric pressure agree considerably better with relevant literature datasets of the highest metrological quality rather than with the EoS.

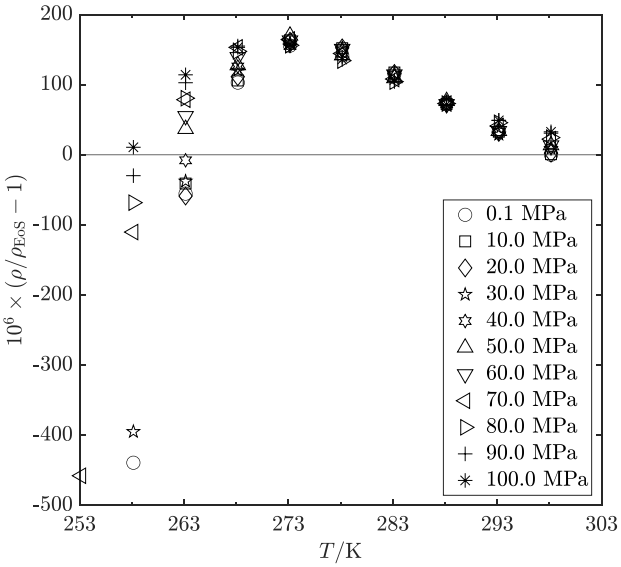

Fig. 7. Relative deviations of D_2O densities from this work from densities calculated wtih equation of Herrig et al.[14].

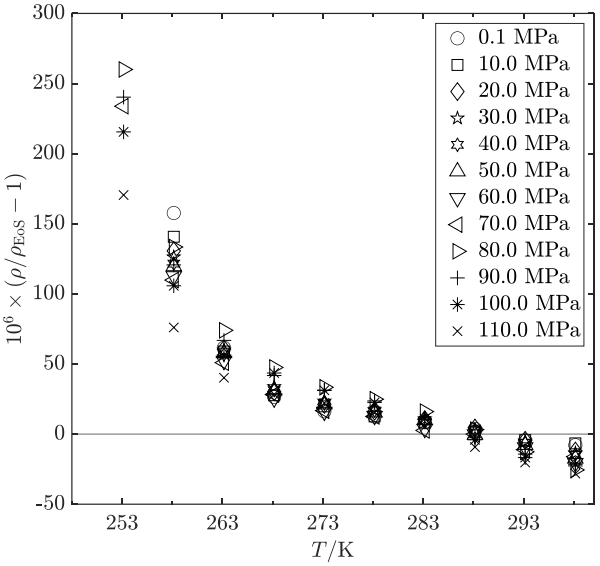

Fig. 8. Relative deviations of seawater densities from this work from densities calculated with TEOS-10 equation [15, 18].

Fig. 8 reveals systematic deviation of our data from reference equation for seawater, TEOS-10. Above melting point temperature, the slope of density vs temperature is slightly different, which is reflected also in the deviation of isobaric expansivities α_p. The deviation in the range of (1 to 2)·10^{-6} K^{-1} is comparable to very small volume thermal expansion coefficient of fused silica. In the stable region the mutual agreement is within experimental expanded uncertainty of our data. In the supercooled region deviations are increasing with decreasing temperature showing thus limited extrapolation capability of TEOS-10.

5.4 Temperatures of maximum density

Water at atmospheric pressure exhibits a density maximum which is located close to 4 °C. The existence of such a density maximum is considered anomalous among all various liquids. However, the same anomalous behavior could be expected for liquids similar to pure water, e.g., dilute aqueous solutions or water isotopologues (water molecules that differ only in their isotopic composition).

As can be seen in figures Fig. 2 to Fig. 4, the density maxima are moving to lower temperatures (and further below the melting point temperature) with increasing pressure. Therefore, measurements in the supercooled region broads the observation range of density maximum phenomenon. E.g., for pure water the density maximum at 30 MPa is already located below the freezing point. Level of supercooling attained in the experiments for pure water enabled to identify density maxima for isobars up to 100 MPa.

In Fig 9. temperatures of maximum density as a function of pressure are compared for water, heavy water and seawater are shown. Temperatures correspond to density maxima in figures Fig. 2 to Fig. 4. However, for evaluating the temperature of maximum density, only relative density data are sufficient. Temperature of

maximum density is then calculated from condition of zero first derivative of relative density. Practically, the particular temperature dependence of relative density may be given by a curve smoothing (or interpolating) experimental data.

Fig. 9 shows interesting feature of three investigated aqueous liquids, i.e. similar evolution of temperatures of density maximum with pressure. The individual pressure dependencies are roughly shifted by just a constant.

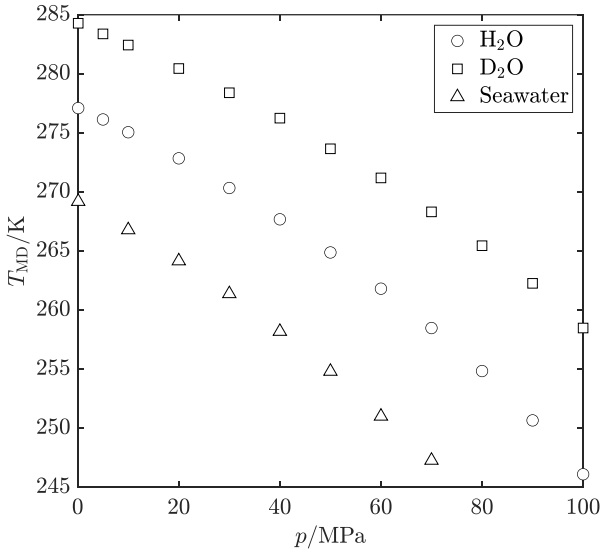

Fig. 9. Comparison of temperatures of maximum density as a function of pressure for all three investigated liquids. Points corresponding to seawater above 40 MPa were calculated from relative densities extrapolated to lower temperatures.

6 Conclusions

As seen the in comparison section 5.3, our results agree well with current reference equations in stable state, but agreement is somehow poorer in the supercooled region. This reflects the fact that validity range of these reference equations (except for Holten equation) is usually from one side limited by the melting curve. The deviation in supercooled region could be thus explained by limited extrapolation capabilities of these equations. At the same time considerable agreement above melting point line validates our experimental method and shows the potential of combining relative density measurement using dual-capillary dilatometer and tool of thermodynamic integration.

The data presented within this contribution may be involved in development of new reference equations of state in order to improve their extrapolation capabilities or improve a description of thermodynamic properties along melting line.

The presented similar course of density maxima for water, heavy water and standard seawater in section 5.4 may be a basis for some future efforts in sense of theorem of corresponding states for aqueous solutions. The reference state would not be a critical point but a curve of maximum density.

Acknowledgement: The study was supported by the Czech Science Foundation grant no. GA19-05696S and the institutional support RVO: 61388998. Dr. Aleš Blahut gratefully acknowledges funding within "Support for International Mobility of Researchers of the Institute of Thermomechanics, Czech Academy of Sciences, part II", no. CZ.02.2.69/0.0/0.0/18_053/0017555 of the Ministry of Education, Youth and Sports of the Czech Republic funded from the European Structure and Investment Funds (ESIF).

References

1. J. Hrubý, J. Hykl, P. Peukert, B. Šmíd, EPJ Web of Conferences 25, 01026 (2012)
2. P. Peukert , M. Duška , J. Hykl, P. Sladký , Z. Nikl, J. Hrubý, EPJ Web of Conferences 92, 02067 (2015)
3. D. E. Hare, C. M. Sorensen , J. Chem. Phys. **87**, 4840 (1987)
4. H. Kanno, C. A. Angell, J. Chem . Phys. **70**, 4008 (1979)
5. O. Mishima, J. Chem. Phys. **133**, 144503 (2010)
6. D. H. Rasmussen, A. P. MacKenzie, J. Chem. Phys. **59**, 5003 (1973)
7. J. V. Leyendekkers, R. J. Hunter, J. Chem. Phys. **82**, 1447 (1985)
8. A. Blahut, J. Hykl, P. Peukert, V. Vinš, J. Hrubý, J. Chem. Phys. **151**, 034505 (2019)
9. K. Fujii, *12th Symposium on Thermophysical Properties (Boulder, Colorado, USA, 1994)*
10. C.-W. Lin, J. P. M.Trusler, J. Chem. Phys. 136, 094511 (2012)
11. K. Meier, A. ElHawary, 17th International Conference on the Properties of Water and Steam (Prague, Czech Republic, 2018)
12. F. Fehres, S. Rudtsch, IAPWSWG-TPWS Meeting (online presentation, 2021)
13. IAPWSR6-95 (2018), Revised Release on the IAPWS Formulation 1995 for the Thermodynamic Properties of Ordinary Water Substance for General and Scientific Use (2018), www.iapws.org
14. S. Herrig, M. Thol, A. H. Harvey, E. W. Lemmon, J. Phys. Chem. Ref. Data 47, 043102 (2018)
15. R. Feistel, Deep-Sea Res. I55, 1639 (2008)
16. F. J. Millero, R. Feistel, D. G. Wright, T. J. McDougall, Deep-Sea Res. I55, 50 (2008)
17. V. Holten, J. V. Sengers, M. A. Anisimov, J. Phys. Chem. Ref. Data 43, 043101 (2014)
18. IOC, SCOR and IAPSO, 2010: *The internationalt hermodynamic equation of seawater --- 2010: Calculation and use of thermodynamic properties. Intergovernmental Oceanographic Commission, Manuals and Guides No. 56, UNESCO (English), 196pp.*